*Materials Sciences and Applications*, **2010, 1, 8-12**
doi:10.4236/msa.2010.11002 Published Online April 2010 (http://www.SciRP.org/journal/msa)

# Temperature Dependence of Current-Voltage Characteristics in Individual $Sb_2Se_3$ Nanowire

**Kien-Wen Sun, Ting-Yuan Fan**

Department of Applied Chemistry, National Chiao Tung University, Hsinchu, Taiwan, China.
Email: kwsun@mail.nctu.edu

Received February 17th, 2010; revised March 11th, 2010; accepted March 15th, 2010.

## ABSTRACT

*We demonstrated techniques toward nanoscale thermometries by using a hydrothermally prepared single $Sb_2Se_3$ nanowire. Suitable electrodes were fabricated to make electrical contact with a nanowire on a silicon substrate by combining techniques of dielectrophoresis, electron beam* (*e-beam*) *lithography, and focused ion beam* (*FIB*). *Measurements of temperature-dependent electrical resistivity were carried out from room temperature up to* 525 *K. The current-voltage characteristics showed linear and symmetric behavior through the entire temperature range, which indicated that the contacts are ohmic. The resistance of the single $Sb_2Se_3$ nanowire decreased with increasing temperature. However, a larger thermal activation energy of ~* 4.2 *eV was found near a temperature above* 420 *K. We speculate that the reduction of resistance at a higher temperature was due to the breakdown of grain boundary barriers.*

***Keywords*: *Nanowire, Dielectrophoresis, E-Beam Lithography***

## 1. Introduction

The measurement of temperature on the nanometer scale is currently a topic of great interest. Advancements in nano- and biotechnology also demand precise thermometry down to the nanoscale. In spatially localized regions of fluid and solid matter, unexpected heat transfer and dynamics in confined nanoscale measurements areas become important. In particular, the performance of modern nanodevices, such as fluidic channels, integrated circuits, and electronic and biologic devices, is often determined by thermal considerations. The development of nanoscale thermal sensing devices can meet the requirement for both accuracy and resolution. Several devices and techniques employing the physical properties of materials, such as their thermal expansion/contraction of volume, thermo-optical and electronic properties, have been developed for the measurement of temperature on the scale of microns and below. For example, the linear thermal expansion behavior recorded for a liquid gallium column confined in the MgO nanotube was used as a nano thermometer in microenviroments [1]. Another common way to measure local temperature is to use a thermocouple, which can be fabricated lithographically or can be vapor-deposited onto nanotips made from another metal [2-5]. A noncontact thermometer with the support of a fiber-optic sensor was demonstrated in [6]. Naberhaus *et al.* [7,8] reported that certain messenger RNAs change their conformation in response to temperature. Kotov *et al.* developed a reversible nano thermometer comprised of a dynamic structure with two types of nanoparticles. These are connected by polymeric spacers acting as a molecular spring in the aqueous state [9].

In recent years, antimony triselenide ($Sb_2Se_3$), a layer-structured semiconductor of an orthorhombic crystal structure, has attracted considerable attention due to its switching effects [10] and good photovoltaic and thermoelectric properties [11,12]. Its high thermoelectric power allows possible applications for optical, thermoelectric cooling, and power conversion devices. In this work, we demonstrate the temperature dependence of a single $Sb_2Se_3$ nanowire's transport properties using dielectrophoresis, E-beam lithography, and focused ion beam (FIB) technique. The thermal properties of this device can be effectively used as a nano thermometer in environments where conventional methods cannot make measurements.

## 2. Experimental Details

Fabrication processes of the single nanowire-based nano thermometer are given as follows. Our $Sb_2Se_3$ nanorod samples were produced from a single source precursor $Sb[Se_2P(O^iPr)_2]_3$ and have been studied and demonstrated elsewhere [13,14] under different solvothermal temperature conditions. The SEM images of the fabric

 

cated nanowire clusters are shown in **Figure 1**. The nanowires have a diameter of 70 nm to 90 nm and an average length of 3 μm to 5 μm. EDS indicates that these nanowires are composed of the element Sb and Se with the ratio of 1:1.5, as shown in **Figure 2**. **Figure 3** shows the HRTEM image of an individual nanowire which reveals that the nanowire is a single crystal and free from dislocation. The fringe spacing of ca. 3.9 Å, 5.2 Å, and 3.2 Å corresponding to (001), (120), and (121) planes of orthorhombic phase $Sb_2Se_3$, respectively. It can be seen that the (001) planes are perpendicular to the surface of the individual nanowire, from which it can be deduced that the wire grew along the [001] direction.

We first diluted the 0.001 g of $Sb_2Se_3$ nanowire powder in 10 ml deionized (DI) water and ethanol mixture. The solution was then placed in an ultrasonic bath operated at a vibration frequency of 185 KHz for 30 min to prevent the formation of clusters. A test drop of the solution was placed on a bare Si wafer, and after the solution dried out, scanning electron microscope (SEM) images were taken to examine the clustering of the nanowires. The concentration of the solution was continuously diluted and adjusted until the nanostructures can be well dispersed on the Si template.

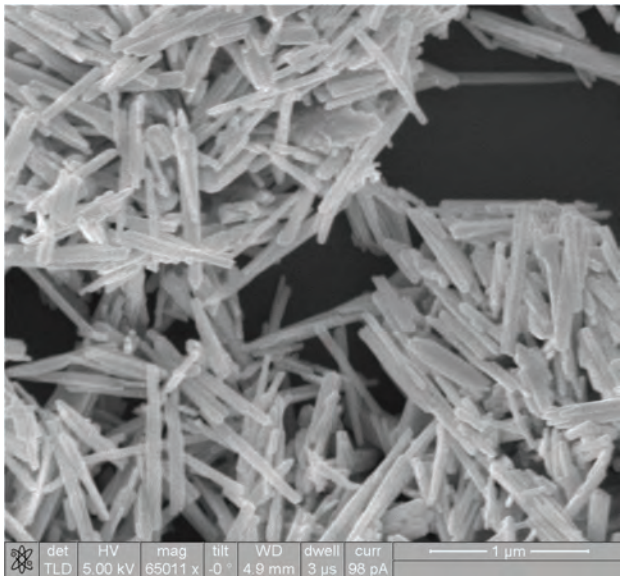


**Figure 1. SEM images of the fabricated $Sb_2Se_3$ nanowire clusters**

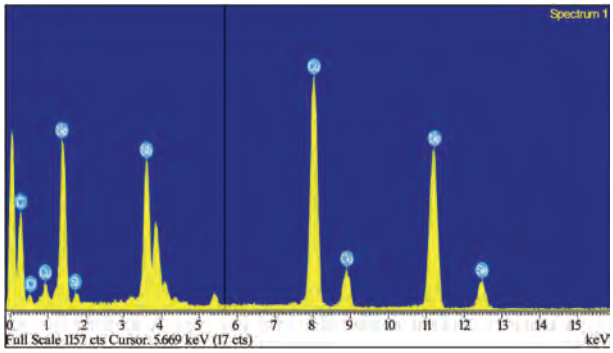


**Figure 2. EDS pattern of the final product (C and Cu signals can be attributed to the copper microgrid and carbon film supporting the $Se_2Se_3$ nanowires)**

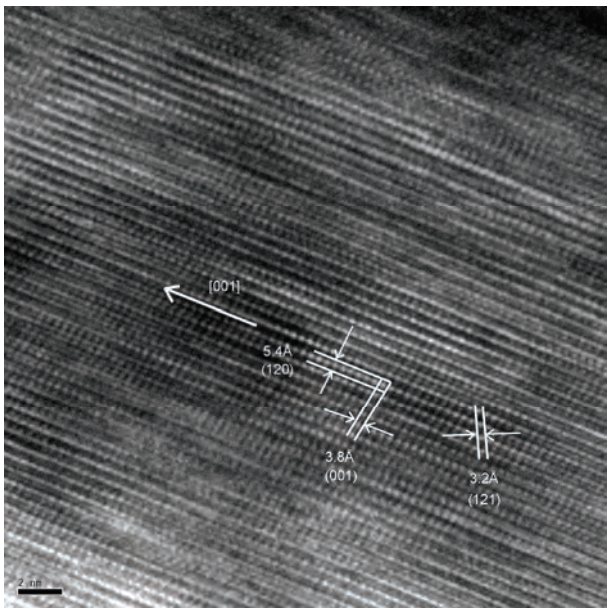


**Figure 3. HRTEM images of an individual nanowire and the corresponding crystal planes**

We designed and fabricated a coordination system on Si templates for labeling a dispersed single nanowire. The templates used in the experiments were commercially available 4-inch silicon wafers with (001) crystal orientation and n-type background doping. The Si wafer was first diced into 2 cm × 2 cm chips. As shown in **Figure 4(a)**, a pattern of two-dimensional arrays of cross-finger-type metal wires with a linewidth of 500 nm, a pitch of 1 μm, and a length of 15 μm were defined on the Si chip using e-beam lithography within an area of 1 $mm^2$.

A drop of diluted $Sb_2Se_3$ nanowire solution was placed within the inter-digitated electrode patterns. By applying a bias across the contact pads, the dielectrophoresis force [15-18] drove the nanowires to bridge the electrode gap. The SEM images of the $Sb_2Se_3$ nanowires' dielectrophoresis alignment process across the inter-digitated electrodes are shown in **Figures 4(b)** and **(c)**. The sample surface was then scanned by SEM to allocate a single nanowire. After a single nanowire was selected, a focus ion beam (FIB) was used to selectively deposit Platinum (Pt) metal contacts on both ends of the rod, as shown in **Figure 4(d)**. The surface of the Si substrate was passivated in advance using a thermally grown $SiO_2$ layer with a thickness of 2000 Å to avoid leakage current

 

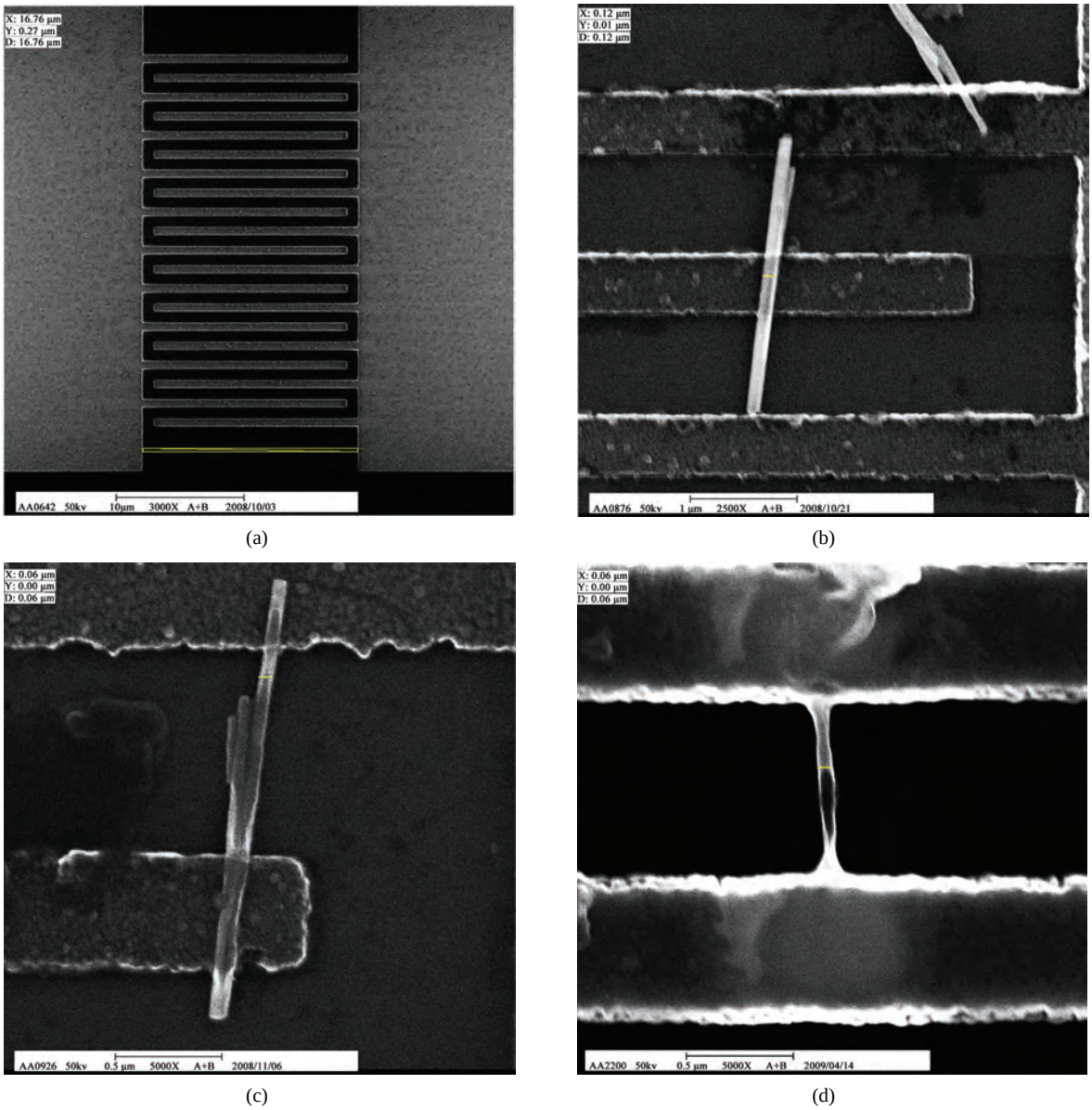


**Figure 4. The SEM images of (a) two-dimensional cross-finger-type metal wire array, (b)-(c) $Sb_2Se_3$ nanowires across the inter-digitated electrodes, and (d) the two-point electrical contact made on a single $Sb_2Se_3$ nanowire**

through the substrate during the current–voltage (I-V) measurements. The temperature dependence of the I-V characteristics of a single nanorod were probed at a temperature range from 300 K to 525 K with an HP-4145 probe station under a current sensitivity of 1 pA and a heating stage.

## 3. Results and Discussion

The electrical contacts were found to be ohmic throughout the scanned voltage range from –0.5 V to 0.5 V with a step of 0.001 V. **Figure 5** shows the I-V curves of a single nanowire from 300 K to 448 K. The resistivity of the nanorod decreased with the increasing temperature due to the increase in free carriers. A thermal activation energy of ~ 0.235 eV was found when the curves between T = 300K to 423K were fitted with the thermally activated transport model [19,20]:

$$R = R_0 \exp(\frac{E_a}{2KT}),$$

where $R_0$ is the resistance at $T = \infty$ and $E_a$ is the thermal activation energy for conduction.

Surprisingly, a dramatic reduction in resistivity was observed when the temperature was increased above 423

 

K, as shown in **Figures 5** and **6**. **Figure 6** shows that the electrical current reaches 170 $\mu$A at the temperature of 523 K and at an applied voltage of 0.5 V. A thermal activation energy larger than 4.0 eV was found when the I-V curves were fitted with the thermally activated transport model. In **Figure 7** we plot the resistance as a function of temperature on a log-log scale. A kink in the curve clearly took place at a temperature of ~ 430 K. The experiments were repeatable when the temperature was cycled from room temperature to 525 K. However, results from temperature dependent Raman, X-ray diffraction, and differential scanning calorimeter measurements ruled out the possibility of phase transition due to the oxidation of the nanorod at a temperature below 525 K. We speculate that the reduction of resistance at a high temperature is due to the escape of trapped charges near the surface. At a high temperature, the breakdown of potential barrier leads to the escape of electrons and holes from the surface traps and results to the carrier transport along the surface and induce an additional quasi-drift current.

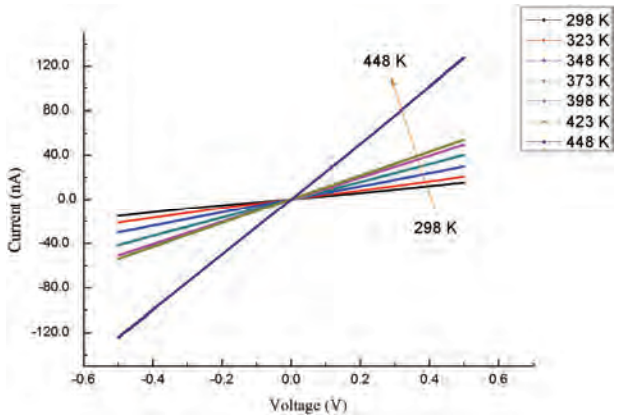


**Figure 5. I-V curves of a two-point contact single nanowire at a temperature range from 300 K to 448 K. The scanned voltage range was from –0.5 V to +0.5 V**

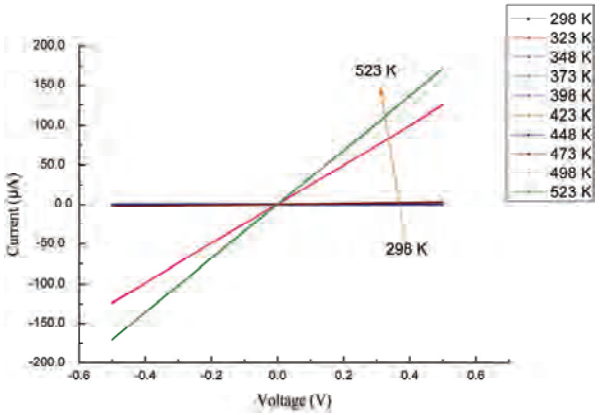


**Figure 6. I-V curves of a two-point contact single nanowire at a temperature range from 300 K to 525 K**

In **Figure 8** a broad PL emission centered at about 700 nm with an FWHM of nearly 150 nm was observed at an excitation wavelength of 532 nm for the single nanorod. The features on this broad emission can be fitted with a single Gaussian peak centered at 675 nm. Although similar PL results were reported by Ma *et al.* [21] on wire-like microcrystalline $Sb_2Se_3$ powder excited with UV laser light. Their experimental results indicated a PL peak at 707 nm but with a much narrower FWHM of only 25 nm. The broad emission peak observed in our experiment originates from the increasing number of surface defects, impurities, and dangle bonds attached to the surface as the dimensions of the nanostructures were reduced from micrometer to nanometer scale. These surface states are clearly responsible for the dramatic increase of electrical conductance at a high temperature.

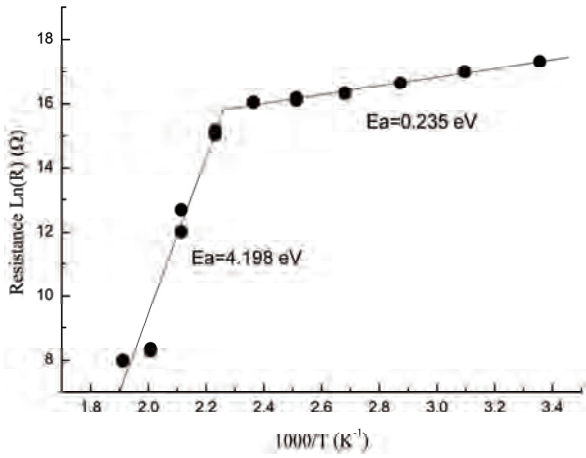


**Figure 7. Resistance as a function of temperature was plotted on a log-log scale. Thermal activated energies of 0.235 eV and 4.198 eV were obtained at the low and high temperature ranges respectively when the I-V curves were fitted with the thermally activated transport model**

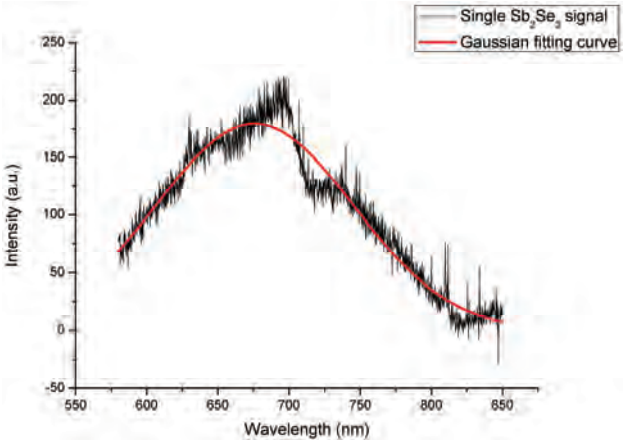


**Figure 8. Photoluminescence spectrum from a single $Sb_2Se_3$ nanowire**

 

## 4. Summary

In conclusion, we demonstrated a novel nano thermometer based on a single $Sb_2Se_3$ nanorod, which can be used for the temperature measurement of a temperature range from 300 K to 525 K, in a micrometer size environment. The temperature dependence of the nano thermometer's transport characteristics shows a dramatic reduction in electrical resistivity (by more than two orders of magnitude) at a temperature near 525 K. The nonlinear electrical behavior of the nanowire is attributed to the grain boundary barrier mechanisms.

## 5. Acknowledgement

This work was supported by the National Science Council of Republic of China under contract No. NSC 96-2112-M-009-024–MY3, and NSC 96-2120-M-009-004-, and the MOE ATU program.

## REFERENCES

[1] Y. B. Li, Y. Bando, D. Golberg and Z. W. Liu, "Ga-Filled Single-Crystalline MgO Nanotube: Wide-Temperature Range Nanothermometer," *Applied Physics Letters*, Vol. 83, 2003, pp. 999-1001.

[2] W. Haeberle, M. Pantea and J. K. H. Hoerber, "Nanometer-Scale Heat-Conductivity Measurements on Biological samples," *Ultramiscroscopy*, Vol. 106, 2006, pp. 678-686.

[3] H. H. Roh, J. S. Lee, D. L. Kim, J. Park, K. Kim, O. Kwon, S. H. Park, Y. K. Choi and A. Majumdar, "Novel Nanoscale Thermal Property Imaging Technique: The 2 ω Method. II. Demonstration and Comparison," *Journal of Vacuum Science and Technology*, Vol. B24, 2006, pp. 2405-2411.

[4] L. Chow, D. Zhou and F. Stevie, "Fabrication of Nanoscale Temperature Sensors and Heaters," U. S. Patent 6905736, 14 June 2005.

[5] Y. Okamura and T. Kohler, "Fabrication of Nanoscale Thermoelectric Devices," U. S. Patent 6969679, 29 November 2005.

[6] H. Aizawa, T. Katsumata, S. Komuro, T. Morikawa, H. Ishizawa and E. Toba, "Fluorescence Thermometer Based on the Photoluminescence Intensity Ratio in Tb Doped Phosphor Materials," *Sensors and Actuators*, Vol. A126, 2006, pp. 78-82.

[7] S. Chowdhury, C. Maris, F. H.-T. Allain and F. Narberhaus, "Molecular Basis for Temperature Sensing by an RNA Thermometer," *European Molecular Biology Organization Journal*, Vol. 25, 2006, pp. 2487-2497.

[8] T. Waldminghaus, A. Fippinger, J. Alfsmann and F. Narberhaus, "RNA Thermometers are Common in α- and γ-proteobacteria," *Biological Chemistry*, Vol. 386, 2005, pp. 1279-1286.

[9] J. Lee, A. O. Govorov and N. A. Kotov, "Nanoparticle Assemblies with Molecular Springs: A Nanoscale Thermometer," *Angewandte Chemie*, Vol. 117, 2005, pp. 7605-7608.

[10] N. S. Platakis and H. C. Gatos, **"**Threshold and Memory Switching in Crystalline Chalcogenide Materials," *Physica Status Solidi*, Vol. A13, 1972, pp. K1-K4.

[11] J. Black, E. M. Conwell, L. Sigle and C. W. Spencer, "Electrical and Optical Properties of Some $M_2$ Ⅴ-B $N_3$ Ⅵ-B Semiconductors," *Journal of Physics and Chemistry of Solids*, Vol. 2, 1957, pp. 240-251.

[12] K. Y. Rajapure, C. D. Lokhande and C. H. Bhosele, "Effect of the Substrate Temperature on the Properties of Spray Deposited Sb-Se Thin Films from Non-Aqueous Medium," *Thin Solid Films*, Vol. 311, 1997, pp. 114-118.

[13] H.-W. Chang, B. Sarkar and C. W. Liu, "Synthesis of $Sb_2Se_3$ Nanowires via a Solvothermal Route from the Single Source Precursor $Sb[Se_2P(O^iPr)_2]_3$," *Crystal Growth & Design*, Vol. 7, 2007, pp. 2691-2695.

[14] Y.-F. Lin, H.-W. Chang, S.-Y. Lu and C. W. Liu, "Preparation, Characterization, and Electrophysical Properties of Nanostructured $BiPO_4$ and $Bi_2Se_3$ Derived from a Structurally Characterized, Single-Source Precursor $Bi[Se_2P(O^iPr)_2]_3$," *Journal of Physical Chemistry C*, Vol. 111, 2007, p. 18538.

[15] K. Yamamoto, S. Akita and Y. Nakayama, "Orientation of Carbon Nanotubes Using Electrophoresis," *Japanese Journal of Applied Physics*, Vol. 35, 1996, pp. L917-L918.

[16] K. Yamamoto, S. Akita and Y. Nakayama, "Orientation and Purification of Carbon Nanotubes Using Ac Electrophoresis," *Journal of Physics D*: *Applied Physics*, Vol. 31, 1998, pp. L34-L36.

[17] W. B. Choi, Y. W. Jin, H. Y. Kim, S. J. Lee, M. J. Yun, J. H. Kang, Y. S. Choi, N. S. Park, N. S. Lee and J. M. Kim, "Electrophoresis Deposition of Carbon Nanotubes for Triode-Type Field Emission Display," *Applied Physics Letters*, Vol. 78, 2001, pp. 1547-1549.

[18] J. Suehiro, G. Zhou and M. Hara, "Fabrication of a Carbon Nanotube-Based Gas Sensor Using Dielectrophoresis and its Application for Ammonia Detection by Impedance Spectroscopy," *Journal of Physics D*: *Applied Physics*, Vol. 36, 2003, pp. L109-L114.

[19] S. M. Sze and K. K. Ng, "Physics of Semiconductor Device," 3rd Edition, Wiley, New York, 2007, pp. 21-25.

[20] R. Smith, "Semiconductors," Cambridge University Press, London, 1980, pp. 18-19.

[21] X. Ma, Z. Zhang, X. Wang, S. Wang, F. Xu and Y. Qian, "Large-Scale Growth of Wire-Like $Sb_2Se_3$ Microcrystallines via PEG-400 Polymer Chain-Assisted Route," *Journal of Crystal Growth*, Vol. 263, 2004, pp. 491-497.

 